Evaluation of Geometric Occlusal Conditions Based on the Image Analysis of Dental Plaster Models

Dominik Grochala[1][0000-0001-9970-710X], *Anna Paleczek*[2][0000-0002-1467-3017], *Justyna Lemejda*[3][0000-0003-0561-9681], *Marcin* Kajor[4][0000-0003-0561-9681], and *Marek* Iwaniec[5][0000 0002 1224 4753]

[1] Faculty of Electrical Engineering, Automatics, Computer Science and Biomedical Engineering AGH University of Science and Technology, Kraków, Poland
[2] Computer Science and Biomedical Engineering AGH University of Science and Technology, Kraków, Poland
[3] Department of Prosthodontics, Institute of Dentistry, Jagiellonian University Medical College, Jagiellonian University, Kraków, Poland
[4] Faculty of Electrical Engineering, Automatics, Computer Science and Biomedical l Engineering AGH University of Science and Technology, Kraków, Poland
[5] Faculty of Mechanical Engineering and Robotics AGH University of Science and Technology, Kraków, Poland

Abstract. It has been proved that dimensions of the dental arch may change as a result of growth or orthodontic treatment. The most intense transformations can be observed at young age during an occurrence of a mixed dentition period. Based on diagnostic models in a form of plaster casts there is a possibility to measure following features: overbite, overjet, the curve of Spee, arch depth, arch width and Bolton's ratios. Nowadays computer-aided tools can provide valuable information for dentists or orthodontists and simplify analysis, diagnosis and preparation of a treatment plan. Correct organization of the dental arch in the horizontal plane can be modelled as a parabola for a mandible and as a section of the ellipse for a jaw. A developed system based on the Python programming language provides automated analysis of plaster model images. Proposed methodology includes preprocessing of provided casts' pictures and segmentation of dental arch using methods such as image morphological operations, edge detection and active contour algorithm. In this research there were also calculated semi-ellipse and parabola fitting functions of dental arches and measured the root mean squared error relative to the original curves. Preliminary results showed 1.29 mm RMSE level for correct occlusion and 2.39 mm in case of malocclusion. Proposed methods can be used for simplifying the analysis of dental arches' shape and monitoring of changes during orthodontic treatment.

1 Introduction

Dental treatment is becoming an increasingly complex process. More and more procedures are becoming involved in diagnostic process. This in turn results in large amount of data

which sometimes is not fully used. For many years, the standard procedure in many cases has been to perform an impression based plaster model as a reliable representation of the patient's tissues and teeth. On the other hand, this approach features several disadvantages, ranging from uncomfortable examination process and difficulties with data archiving to labor-intensive measurements[1]. The use of digital techniques to analyze and archive dental models seems a very promising approach. The application of a 3-D laser scanner allows to digitize plaster models. On the other hand a usage of specialized software allows further analysis. This solution gives good geometrical representations providing information not worse than manually selected physical models[2]. The same result occurs in case of scans made directly in patient's mouth. The measurements obtained in this way correspond to the plaster models. This is also a current direction in development of 3D imaging techniques of oral cavity which is replacing traditional solutions, thanks to the ease of application[1]. Methods based on ionizing radiation can help in digital diagnosis and dental treatment planning. Precise results are provided by the CBCT (Cone-Beam Computed Tomography) a technique which is more and more widely available and willingly used by orthodontists and dental prosthetists. Results obtained in this way are also diagnostically useful on par with traditional models [3]. Nowadays a widespread access to medical facilities is limited due to the increasing number of patients. Nonetheless, modern technology aims to solve this problem by forcing medical procedures to be carried out remotely which directly drives the development of telemedicine and teledentistry[4, 5]. This approach promotes a usage of digitized diagnostic data as well as electronic medical documentation.

Taking alginate impressions are common in daily dental practice. During the first patient's visit to the doctor's office, impressions and plaster models are often made to plan further treatment objectives [6]. They are used by clinicians in numerous cases, some of them being: classification of malocclusions, identification the morphology and position of in dental arches, measurements, designing orthodontic devices (e.g. dental aligners) and prosthetic treatment (for example dentures). Plaster casts are also needed in temporomandibular disorders treatment with dental splints. They can also be used by students of dentistry for learning. There are various techniques and materials utilized in forming of these models, the most popular being alginate (irreversible hydrocolloid). This solution is easily accessible, simple in use, well known and cheap [7].Despite being very useful tool, dental impressions are prone to damage. Unfortunately, frequent use of models may cause wear, abrasion of the material and thus reduce the resistance sometimes resulting in cracking of the model. Another downside is the need to allocate space for storing models [8]. Nowadays, development of new technologies makes digital models more and more popular and begins to replace traditional solutions. The existing plaster models can also be scanned to provide digital representation [9]. Based on plaster models, it is possible to determine the shape and width of the dental arch, transverse symmetry, anterior-posterior symmetry and orthodontic measurements. One of the measurements is the Bolton ratio, which determines the relationship between the sum of the mesiodistal widths of the maxillary and mandibular permanent teeth, enabling the determination of the harmony of the dental arch. The shape of the mandible dental arch is similar to a parabola [10–12]. The upper arch has a shape of ellipse or semi-ellipse [12–15]. In 1975 Lavelle performed the measurements of plaster models based on alginate impressions of the maxillary and mandibular arches. The studied casts belonged to people between 4 and 20 years from ethnic groups of Caucasoids, Mongoloids and Negroids. The number of used plaster models was 2040. The researcher measured among others dental arch width and length. Burris et. al. examined the arch form in American blacks and whites to help understanding differences in tooth crown dimensions, dental crowding etc. at various ethnic groups. The

researchers used the dental study casts from 330 patients. All participants had full complement of natural teeth but not orthodontically treated. 18 measurements points were marked on the dental casts and then used as coordinates to set the arch curve. The results showed that the blacks has larger arch widths and depths than whites [16].Kanavakis et. al. conducted a study of patients with temporomandibular joint disorders to assess the differences in the occlusal curvature and the dimensions of the dental arch. The study included 100 participants, 78 female and 22 male. The occlusion measurements were performed on plaster models with a digital caliper and the temporomandibular disorders were classified with the Research Diagnostic Criteria in Temporomandibular Disorders questionnaire. The depth of the curve of Spee and the depth of curve of Wilson were also measured [17].As plaster models, despite being imperfect, still constitute the basis of prosthetic and orthodontic work. Combining this fact with the need to digitize the whole approach to take advantage of automatic analysis methods there have been proposed a simple system for visual evaluation of traditional models.
Its undoubted advantage is the ease of acquiring images and their quick evaluation with the use of tailored image recognition algorithms.What is more, plaster models are created at as intermediate stages of other procedures and therefore using them for additional analysis allows better use of already diluted diagnostic data.
Nowadays more and more is taking advantage of image processing algorithms which are developed to solve advanced computer vision tasks. Those applications are designed to acquire, process and analyze digital images or videos. Obtained results can be used to classify objects, measure object morphometric parameters such as width, height, volume, circumference and recognize objects or reconstruct data. The most popular and commonly used algorithms include basic and advanced image preprocessing methods such as foreground extraction, feature detection, noise reduction, image filtration, object segmentation and edge detection [18–21]. State-of-art and popular mathematical method called photographometry is based on the dental plaster photos taken at different angles of camera. This algorithms generates 3D coordinates of the object. Those points are used to create three-dimensional grid of the object and reconstruct digital 3D model from traditional photos. In this case, a comparative evaluation of automatic digital models measurements in the context of traditional dental plasters evaluation (tooth width and height) results in the accuracy of -0.4 to 0.6 mm[22]. Current modern applications are actually developed to works with complex 2D and 3D medical images. Prepared visualizations and obtained results are useful for doc-tors during diagnosis, planning treatment, assessing treatment results and storing or sharing images to consult remotely with other specialists.

2 Materials and methods

Plaster models were made from alginate impressions, which were used during dental diagnostics. Total number of 20 volunteers, including authors, participated in this study. Subjects included in the research may have had orthodontic treatment in the past. Utilized dental formula was at least one molar, one premolar, canine, and two incisors in each quadrant. A poor quality of diagnostic models was chosen as the exclusion criteria. The model casts were provided together with individual, fully anonymised identification numbers.
In the last stage, quantitative data obtained from computational models was compared with the diagnosis made by the dentist, which were also presented in an anonymised form, using consistent numbering. The total number of tested models were 20 pairs (maxilla and

mandible) - each pair was taken from independent patients. 18 models were left for further analysis due to significant mechanical damage and two impressions were fully rejected.

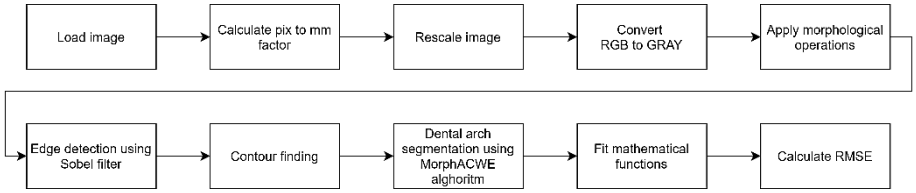

Fig. 1. Image processing algorithm described used in this paper.

The algorithm presented in this paper was developed using Python language with popular scientific libraries one of them being Scikit-image [23], which contains popular algorithms used for image processing. Another utilized package was SciPy[24], which is well-known collection of various, advanced numerical functions such as optimisation, signal processing, statistic etc. Proposed algorithm also takes advantage of Scikit-learn [25] module, which includes score functions, performance metrics, machine learning tools and algorithms and NumPy[26] - a library providing advanced means of numerical computations. In turn, Visualisation of obtained results was implemented with Matplotlib package [27].

The general block diagram of image processing algorithm proposed in this paper is shown in the (Fig.1).

To calculate the conversion factor between pixels and millimeters, there were used two methods. The first one is based on taking photos of the scene containing plaster model together with a small red rectangle with a well-defined area placed nearby (Fig.2a). It is a fully-automated calibration method, but its main disadvantage is a high dependence on the angle of used camera. On the other hand the manual method was used to obtain higher accuracy by drawing a line on the taken picture and entering the length of the line in millimeters (Fig.2b).

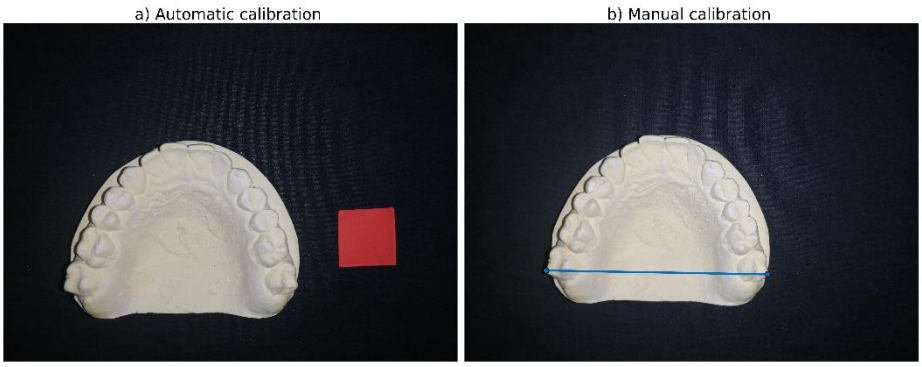

Fig. 2. Comparison of two calibration methods a) Automatic calibration using a small red square indicator, b) Manual calibration using a line drawn on the picture.

Pictures of the dental plasters were taken using a standard digital camera with a resolution of 5120x3840. Obtained photos were preprocessed – rescaled and converted from RGB image into a grayscale. The dental plaster object was segmented using the global threshold

function. It was done in order to remove background and the red square indicator if automatic calibration method was used. Then, morphological operations such as binary erosion, binary dilation and removal of small object function were performed. As a next step of image processing the Sobel filter was applied to the pictures to enhance and detect edges.

The Sobel filter [28] is commonly used to calculate the X and Y partial derivatives on the image. This method is applied to extract edges and objects' boundaries in the input picture. The Sobel operator consists of two 3 x 3 kernels (eq.1) which are used for performing convolution operation on the image.

$$\begin{bmatrix} -1 & 0 & +1 \\ -2 & 0 & +2 \\ -1 & 0 & +1 \end{bmatrix} \begin{bmatrix} +1 & +2 & +1 \\ 0 & 0 & 0 \\ -1 & -2 & -1 \end{bmatrix} \tag{1}$$

Gx Gy

Output image is a combination of two separate images - results of the convolution using Gx and Gy operators. To find output values of each pixel an absolute gradient magnitude (norm of each pixels X and Y partial derivatives) is calculated at each point (eq.2). There is also a possibility to calculate a gradient direction (eq.3).

$$|G| = \sqrt{{G_x}^2 + {G_y}^2} \tag{2}$$

$$\theta = arctan\left(\frac{G_y}{G_x}\right) \tag{3}$$

The results of applying the Sobel filter were presented in the (Fig.3)

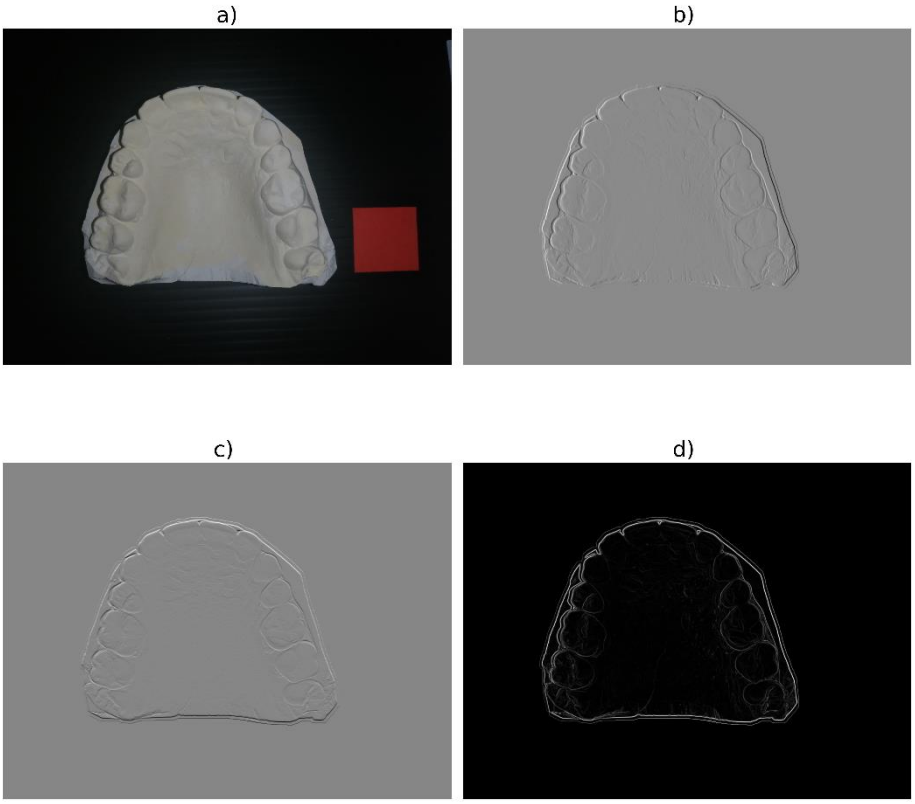

Fig. 3. The application of Sobel filter. a) Input image, b) Convolution with Gx operator, b) Convolution with Gy operator, d) Calculated gradient magnitude.

To find contours of the dental arches a Contour Finding Function from scikit-image library was used. Due to the similar color of the entire plaster model and insufficient distinguishing of the contours of the dental arch, the Morphological Active Contours without Edges (MorphACWE) algorithm [29] was applied. This method is commonly used for segmenting objects in pictures without well-defined contours. For the obtained contours of the Maxillary dental arch and Mandibular dental arch, a half-ellipse (eq.4) [30] and a parabola (eq.5) functions were fitted respectively.

$$x = a \cdot \cos(t) \cdot \cos(\theta) - b \cdot \sin(t) \cdot \sin(\theta) + x_c$$

(4)

$$y = a \cdot \cos(t) \cdot \sin(\theta) + b \cdot \sin(t) \cdot \cos(\theta) + y_c$$

The root mean squared error (eq.6, eq.7) between the original and the fitted curve was also calculated.

$$MSE(y, \hat{y}) = \frac{1}{n_{samples}} \sum_{i=0}^{n_{samples}-1} (y_i - \hat{y}_i)^2 \quad (5)$$

$$RMSE(y,\hat{y}) = \sqrt{\frac{1}{n_{samples}}\sum_{i=0}^{n_{samples}-1}(y_i - \hat{y}_i)^2} \quad (6)$$

Bolton Analysis

$$B_{anterior} = \frac{S_{6\ mamd}}{S_{6\ max}} \quad (7)$$

$$B_{overall} = \frac{S_{12\ mamd}}{S12_{12\ max}} \quad (8)$$

3 Results

The algorithms and application described in the previous chapter were implemented and the input was provided as a set of photos to verify the system's operation. The output data was constituted by the calculated measures of similarity, coefficients and visualized additions in the form of graphs. In the final step, the RMSE values were compared with the standard diagnoses (Table 1.). The diagnostic information included: Angle's classification(Class), teeth topography disorders(correct / incorrect) and teeth missing(yes / no).
The two exemplary visualizations were chosen of the results of processing images of the dental plaster models. For each of these two models, the original photos of the upper and lower arcs were compiled together with a segmented (maxillary and mandibular) dental arch and the corresponding curves fitted. Fig.4 shows plaster cast of people who have had orthodontic treatment and Fig.5 shows dental model with visible malocclusion.

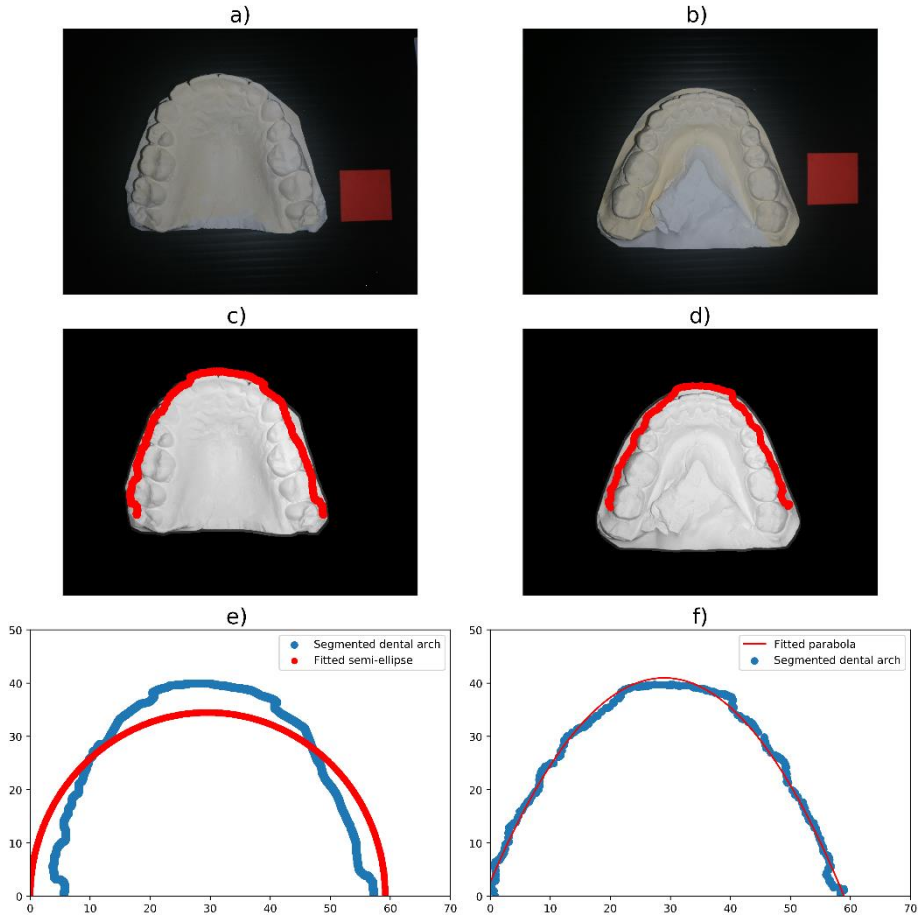

Fig. 4. Dental plaster no 22. a) Input photo of the maxilla model, b) Input photo of the mandible model, c) Maxillary dental arch segmentation, d) Mandibular dental arch segmentation e) Segmented upper dental arch with fitted semi-ellipse function f) Segmented lower dental arch with fitted parabola function.

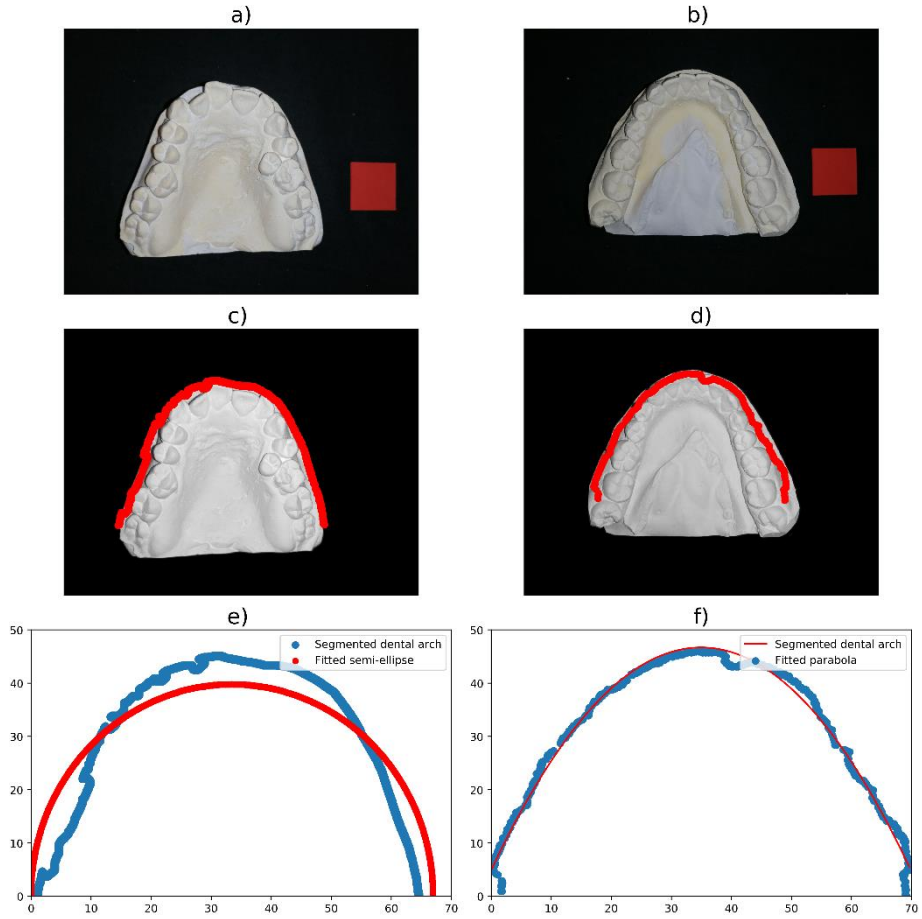

Fig. 5. Dental plaster no 26. a) Input photo of the maxilla model, b) Input photo of the mandible model, c) Maxillary dental arch segmentation, d) Mandibular dental arch segmentation e) Segmented upper dental arch with fitted semi-ellipse function f) Segmented lower dental arch with fitted parabola function.

Bolton Analysis were calculated as an additional parameter that could be determined using the proposed algorithms. The anterior (eq.8) and overall (eq.9) Bolton ratios were calculated using segmented maxillary and mandibular dental arches. Obtained results were presented in (Table 1) for individual models.

Table 1. Calculated similarity coefficients of analyzed models with idealized arch geometry curves.

No. model	Diagnosis	Maxillary dental arch		Mandibular dental arch		Bolton Anterior	Bolton Overall
	Angle's class / topography / teeth missing	Width [mm]	RMSE [mm]	Width [mm]	RMSE [mm]	[%]	[%]
2	Class II division 2 / incorrect / no	70	3.85	64	3.06	97.05	98.49
10	Class II division 1 / incorrect / no	64	5.03	59	1.63	91.11	95.70
13	Class I / incorrect / yes	56	5.18	61	3.10	84.26	93.35
14	Class II division 1/ incorrect / no	60	4.52	59	2.80	93.33	112.96
15	n/a / incorrect / yes	52	2.63	66	1.25	75.00	87.36
17	Class I / incorrect / yes	54	4.05	64	1.31	80.10	94.64
18	n/a / incorrect / yes	60	3.49	52	2.42	82.91	90.79
19	Class I /correct / no	67	4.97	64	2.28	77.55	92.21
21	Class I / incorrect/ no	61	6.00	64	2.79	81.84	97.20
22	Class I /correct / yes	61	4.76	59	1.29	86.63	96.44
24	Class I / incorrect/ no	63	5.15	63	2.43	71.64	88.97
26	Class III / incorrect/ no	68	6.55	69	1.78	77.13	105.10
30	Class I / correct / no	64	3.69	61	1.79	64.26	78.34
32	Class I / incorrect / no	60	4.43	62	2.48	89.93	86.47
33	Class I / correct / no	65	6.19	58	2.13	79.16	93.75
36	Class II division 2/ incorrect / yes	54	4.05	54	2.39	77.52	98.49
101	Class I / correct / yes	58	2.92	64	1.42	78.18	100.24
102	Class II / incorrect / yes	63	4.65	64	2.13	123.90	132.35

4 Discussion and Conclusions

In this paper there have been proposed and implemented a methodology of accessing the correctness of the dental arch geometry. It should be noted that this approach is a significant simplification of the analysis in the horizontal plane of the dental arch projection, as there are many geometric dependencies in orthodontic and prosthetic treatment. Also, in order to increase the reliability of the algorithm the fitting method of the curve approximating the spacing of the teeth was based on the detection of outer edges and not the centers of the teeth. Thanks to this solution, it is also possible to calculate indicators such as Bolton's ratio using the same image processing application.

The presented approach is simple to use because of being based on taking a regular photos with the use of an easily accessible camera instead of an expensive 3-D scanner. This allows for the additional use of diagnostic models, which are often abandoned in the diagnostic or treatment process, and constitute an additional source of diagnostic information. Moreover, such a solution provides a simple tool for more accurate analysis of the dental arch which may support inexperienced dentists in case of limited access to specialists. Wędrychowska-Szulc et. al. also determined the Bolton index, however, the method of determination was different from the method presented in this article. Despite this, the obtained results for Angle class and Bolton overall values were similar [31]. The newest research of Suryajaya et. al. confirmed the compatibility of using digital solutions. Moreover the conclusion is that digital and printer models may replaced conventional plaster model to modern denouement [32].

Sridharan et. al. did not notice the differences in measurements quality of plaster and digital models [33].

The use of ordinary photos taken without a tripod and dedicated equipment is quick and convenient, but on the other hand it introduces many limitations, such as image distortions, which constituted an additional challenge during image processing and scaling.Bolton measurements are highly dependent on the correctness and accuracy of the tooth arch segmentation. Incorrect detection of tooth edges, in some cases, could result in inaccurate calculation of the coefficients. Another drawback of the presented algorithm was that the length of the arch between the respective teeth was calculated, instead of the width of the individual teeth.Ellipse and parabola standard curves fitting approach is also very prone to error resulting from incomplete dentition, and results in significantly erroneous results. For example model number 15 and 17 shows a very low RMSE error with concomitant topology disturbance. It is a result of corresponding teeth missing.With an exception of the analyzed case 22. where, despite the actual lack of teeth, the remaining ones are positioned correctly in the arch thanks to orthodontic treatment, which is recognized by the algorithm as correct dentition. Large inconsistency were noticed in arc fitting to a semi-ellipse. It seems that the mentioned standard curve is a reference only in some cases, and it would be more effective to fit defined segment of an ellipse.Therefore more attention was paid to the Mandibular dental arch analysis

Presented system might be imperfect, but it shows promising prospects for further development, including implementation of the functionality of calculating additional parameters or increasing the resistance to distortions on input photos. Despite some simplifications, used methodology, provided RMSE result correlated with the diagnosed topography disturbance performed in a traditional, manual way. Obtained data allows to determine the deviation from the adopted model curves, which corresponds to the actual assessment of the dental arches and their possible pathologies. As an example of a correct topology of the dental condition, there were takena model 22 as opposed to 36, where the algorithm was calculated without significant interference, such as missing teeth. Moreover,

the correct Bolton index for case 36 indicates an independent occurrence of disturbances in topography and interarch relationship.
Kurt et. al. took an impresions from 18 patients and did the plaster models. The plaster models were scanned and the researchers calculated Bolton ratio in conventional and digital way. Subsequently the scientists compared the results of both solutions. The conclusion was high accuracy and reliability of used methods [34].
Finally, the implementation of designed system as a mobile application running on a smartphone would provide a ready-made tool for dentists to facilitate a more accurate examination of patients with the use of common models. Therefore, it seems reasonable to continue research and develop the project as an easily accessible supplement to the current standards in dentistry.

References

1. F. Zhang, K.-J. Suh, K.-M. Lee Validity of intraoral scans compared with plaster models: an in-vivo comparison of dental measurements and 3D surface analysis (2016).
2. R.P. Reuschl, W. Heuer, M. Stiesch, D. Wenzel, M.P. Dittmer Reliability and validity of measurements on digital study models and plaster models (2015).
3. C. Lippold, C. Kirschneck, K. Schreiber, S. Abukiress, A. Tahvildari, T. Moiseenko, G. Danesh Methodological accuracy of digital and manual model analysis in orthodontics–A retrospective clinical study (2015).
4. S.J. Daniel, S. Kumar Teledentistry: a key component in access to care (2014).
5. A. Bhambal, S. Saxena, S.V. Balsaraf Teledentistry: potentials unexplored, (2010).
6. V.V. Nandini, K.V. Venkatesh, K.C. Nair Alginate impressions: A practical perspective (2008).
7. C. Paganelli, G. Gastaldi, G. Denotti, A. Piras, G. Spoto, A. Scarano, M. Petrini, M. Ferrante, S. Catapano, N. Mobilio Materiali e tecnologie odontostomatologiche per igienista dentale (2013).
8. M.J. Peluso, S.D. Josell, S.W. Levine, B.J. Lorei Digital models: an introduction (2013).
9. T. Grünheid, N. Patel, N.L. De Felippe, A. Wey, P.R. Gaillard, B.E. Larson Accuracy, reproducibility, and time efficiency of dental measurements using different technologies, (2014).
10. M. Jones, S. Richmond An assessment of the fit of a parabolic curve to pre-and post-treatment dental arches (1989).
11. H. Sicher, E.L. DuBrul Oral anatomy (1975).
12. I. Karłowska Zarys współczesnej ortodoncji: podręcznik dla studentów i lekarzy stomatologów (2001).
13. F.L. Stanton Arch predetermination and a method of relating the predetermined arch to the malocclusion, to show the minimum tooth movement (1922).
14. G. Izard New method for the determination of the normal arch by the function of the face (1927).
15. D.D. Chung, R. Wolfgramm Maxillary arch perimeter prediction using Ramanujan's equation for the ellipse (2015).
16. B.G. Burris, E.F. Harris, Maxillary arch size and shape in American blacks and whites (2000).
17. G. Kanavakis, N. Mehta The role of occlusal curvatures and maxillary arch dimensions in patients with signs and symptoms of temporomandibular disorders (2014).
18. M.A. Alzubaidi, M. Otoom A comprehensive study on feature types for osteoporosis classification in dental panoramic radiographs (2020).

19. T. Pun, G. Gerig, O. Ratib Image analysis and computer vision in medicine (1994).
20. E. Avuçlu, F. Başçiftçi The determination of age and gender by implementing new image processing methods and measurements to dental X-ray images (2020).
21. A. Chen, L. Zhu, H. Zang, Z. Ding, S. Zhan Computer-aided diagnosis and decision-making system for medical data analysis: a case study on prostate MR images (2019).
22. V.T. Stuani, R. Ferreira, G.G. Manfredi, M.V. Cardoso, A.C. Sant'Ana Photogrammetry as an alternative for acquiring digital dental models: A proof of concept (2019).
23. S. Van der Walt, J.L. Schönberger, J. Nunez-Iglesias, F. Boulogne, J.D. Warner, N. Yager, E. Gouillart, T. Yu Scikit-image: image processing in Python (2014).
24. P. Virtanen, R. Gommers, T.E. Oliphant, M. Haberland, T. Reddy, D. Cournapeau, E. Burovski, P. Peterson, W. Weckesser, J. Bright SciPy 1.0: fundamental algorithms for scientific computing in Python (2020).
25. F. Pedregosa, G. Varoquaux, A. Gramfort, V. Michel, B. Thirion, O. Grisel, M. Blondel, P. Prettenhofer, R. Weiss, V. Dubourg Scikit-learn: Machine learning in Python (2011).
26. T.E. Oliphant A guide to NumPy (2006).
27. J.D. Hunter Matplotlib: A 2D graphics environment (2007).
28. J.D. Bakos Embedded Systems: ARM Programming and Optimization. Morgan Kaufmann (2015).
29. P. Marquez-Neila, L. Baumela, L. Alvarez A morphological approach to curvature-based evolution of curves and surfaces (2013).
30. R. Halır, J. Flusser Numerically stable direct least squares fitting of ellipses (2013).
31. B. Wędrychowska-Szulc, J. Janiszewska-Olszowska, P. Stepień Overall and anterior Bolton ratio in Class I, II, and III orthodontic patients (2010).
32. W. Suryajaya, M. Purbiati, N. Ismah Accuracy of digital dental models and three-dimensional printed dental models in linear measurements and Bolton analysis. F1000Research. 10, 180 (2021).
33. S. Sridharan, S.A. Kumar Model analysis: Plaster versus computer-assisted photographic model assessment-A prospective clinical study. Drug Invent. Today. 11, (2019).
34. N.G. Amuk, E. Karsli, G. Kurt Comparison of dental measurements between conventional plaster models, digital models obtained by impression scanning and plaster model scanning. Int. Orthod. 17, 151–158 (2019).